Brazilian Journal of Experimental Design, Data Analysis and Inferential Statistics

Federal University of Rio de Janeiro
BJEDIS, Rio de Janeiro, Special Edition, v. 01 (2), 2021
DOI: https://doi.org/10.55747/bjedis.v1i2.48358
ISSN: 2763-6925

**Special Edition** **Received 02/04/2021. Revised 03/15/2021. Accepted 04/20/2021. Published 07/01/2021.**

# Effective immunization scenarios by vaccination against COVID-19 obtained through Bayesian analysis

Hanniel Ferreira Sarmento de Freitas*[1,2], Paulo Henrique Soares[1,3] and Cid Marcos Gonçalves Andrade[1]

*[1]State University of Maringá, Maringá, Brazil; [2]Federal Institute of Education, Science and Technology of Rio Grande do Norte – Nova Cruz Campus, Nova Cruz, Brazil; [3]Federal Technological university of Paraná - Guarapuava Campus, Guarapuava, Brazil;*

**Abstract:** The COVID-19 pandemic caused a health crisis on an unprecedented scale, due to the unstoppable spread of the disease through the global integration provided by the current strongly globalized society. Isolation policies recommended by WHO impacted countries economies, making it necessary to implement a range of economic, health, social and economic security policies, such as: financial aid packages for the population and companies, investment of resources for the structuring of hospital beds for the treatment of patients, implementation of population testing programs, among others. The impact of the pandemic proved to be quite significant especially for the so-called "developing countries", due to the difficulties in establishing the aforementioned range of security policies as well as mass testing of the population in order to reliably map the disease spreading. The implementation of those measure were limited not only by economic reasons, but also by political impediments. In the present study, a Bayesian analysis of the immunization rate against COVID-19 through vaccination, evaluating the immunization scenarios lasting or temporary. The logistics required for the vaccination campaign in Brazil were assessed by considering uncertainties in determining the daily rate of immunization, as well as the effectiveness of the vaccine made available for the population. In this intent, an epidemiological model was used compartmentalized, calibrated against historical data using the CATMIP stochastic algorithm. The obtained results indicate that the daily vaccination rate is the most important parameter of a successful immunization program, given an effectiveness rate equal or superior to 50%. However, a massive immunization rate needs to be conjugated with a responsible relaxing of the social distancing measures after the vaccination program start, under the risk of compromising any positive result in terms of the number of contaminated and deceased individuals.

**Keywords:** COVID-19; epidemiologic modeling; bayesian calibration

**Adherence to the BJEDIS' scope:** This work is related to the scope of BJEDIS as it presents a predictive analysis for COVID-19 disease transmission in Brazil.

*Federal Institute of Education, Science and Technology of Rio Grande do Norte - Nova Cruz Campus, José Rodrigues de Aquino Filho Av., 640, Alto de Santa Luzia, 59215-000, Nova Cruz, Brazil; E-mail hanniel.freitas@ifrn.edu.br

## 1. INTRODUCTION

The COVID-19 is a pandemic that has spread rapidly in almost the totality of the countries of the world, arising serious concerns in the sanitary authorities and in the society in general. Even one year after the first case in the Chinese city of Wuhan, several countries still present epidemiological data that are not at all reliable, considering the lack of population mass testing capacity (especially in the so called "developing countries"), as well as clinical characteristics intrinsic to the disease, which include long incubation period with symptoms absence and a great number of asymptomatic carriers (1-3). Those inconsistencies are translated in uncertainties in the epidemiological data, which need to be considered during the task of modeling the disease spreading process, especially for future scenario projections.

After the Brazilian population witnessed an escalation in the number of deaths due to COVID-19, which proved to be subsidized by the difficulty in establishing the effective social distance and prophylactic care as frequent hand hygiene, and most recently the low vaccination rate. Those measures consist of the only concrete measures for coping with the disease in the present moment, considering the nonexistence of a pharmacological treatment for it according to the World Health Organization (WHO), although part of the Brazilian institutions have endorsed the use of drugs without proper support from the authorities competent medical practitioners. However, the development and availability of vaccines for coping of the disease - an unprecedented feat in science in terms of its speed - presents itself as a reliable alternative for coping with COVID-19. In this sense, there are two uncertainties regarding the immunization response vaccination: the logistical capacity of provide immunization for the population, and the duration of immunization provided by it. The present work aims to develop a modeling for the process of transmission of COVID-19 considering the uncertainties from the registration of epidemiological data and analyze scenarios for the variables already mentioned in regards vaccination.

## 2. METHODOLOGY

### 2.1 Epidemiological modeling of the problem

In modeling the COVID-19 transmission process in the country a compartmentalized epidemiological model was used, based in the work of (1, 2, 4) with the consideration of social distance between individuals. Thus, individuals can be divided into the following compartments: susceptible (S) to infection; exposed (E), the which have had contact with the viral agent and will become carriers of the virus (symptomatic or not); infected symptomatic (I), although not yet officially detected as contaminated; asymptomatic infected (A), which have low viral load and therefore symptoms that do not justify the search for medical care, even though they are capable of transmitting the disease; infected individuals tested (T), who are assumed to have sought medical care, since the expressive majority of tests in the country are carried out only when such a situation occurs; individuals already recovered (R), who managed to recover from the disease and remain immune to it for a certain period of time; individuals who died (D) as a result of disease and/or its complications; individuals immunized by vaccination (V), which require an specific amount of time for developing immunological capabilities against the *Sars-CoV-2* virus, and will remain immune to the disease until that immunity is reduced below a critical value. The model was called *MOSVAC* (*SEIARD* model with Vaccination), which can be expressed according to Equations 1-8.

$$\frac{dS}{dt} = -\beta\frac{S}{N}(I + \kappa A) - \sigma S + \Lambda(V)\left(\theta_V V - \lambda\frac{\Phi}{N}\Psi S\right) \quad (1)$$

$$\frac{dE}{dt} = \beta\frac{S}{N}(I + \kappa A) - (\nu + \sigma)E \quad (2)$$

$$\frac{dI}{dt} = \rho\nu E - (\epsilon_I + \gamma_I + \eta_I + \sigma)I \quad (3)$$

$$\frac{dA}{dt} = (1 - \rho)\nu E - (\epsilon_A + \gamma_A + \eta_I + \sigma)A \quad (4)$$

$$\frac{dR}{dt} = \gamma_A A + \gamma_I I + \gamma_T T + \sigma(S + E + I + A)A - \theta_R R \quad (5)$$

$$\frac{dD}{dt} = \eta_T T + \eta_I I \quad (6)$$

$$\frac{dT}{dt} = \epsilon_I I + \epsilon_A A - (\eta_T + \gamma_T)T \quad (7)$$

$$\frac{dV}{dt} = \Lambda(V)\left(\lambda\frac{\Phi}{N}\Psi S - \theta_V V\right) \quad (8)$$

The relevant parameters for *MOSVAC* model are presented in the Table 1, in which the meaning of each one in the compartmentalized modeling context is presented. It is important to notice that it is assumed that the possibility for the transmission of the disease from the vaccinated individual during the time of proper immunity development, as suggested by sanitary authorities (5).

**Table 1.** *MOSVAC* model parameters and their respective meanings, along with values and units, when relevant.

| Parameter | Value | Units | Meaning |
|---|---|---|---|
| $\beta$ | Calibrated | $days^{-1}$ | Daily rate of effective contacts for disease transmission |
| $\nu$ | 1/5 | $days^{-1}$ | Inverse of the time for symptomatic manifestation |
| $\kappa$ | 1 | - | Proportionality factor between for asymptomatic and symptomatic individuals contact rate |
| $\gamma_I = \gamma_T, \gamma_A$ | Calibrated; 1/14 | $days^{-1}$ | Inverse of the time for recovery from the disease |
| $\eta_I = \eta_T$ | 0.1% | $days^{-1}$ | Disease daily fatality rate |
| $\sigma$ | Calibrated | $days^{-1}$ | Daily rate of social distancing |
| $\rho$ | 85% | - | Percentage of symptomatic carriers |
| $\epsilon_I = \epsilon_T, \epsilon_A$ | Calibrated; 1/5 | $days^{-1}$ | Inverse of the time for disease detecting through testing |
| $\Lambda(V)$ | 0 or 1 | - | Parameter for signaling the occurrence (1) or absence (0) of vaccination |
| $\Psi$ | Projected | $days^{-1}$ | Immunization effectivity through vaccination |
| $\Phi$ | Projected | $days^{-1}$ | Daily rate of immunization of individuals |
| $\theta_V$ | Projected | $days^{-1}$ | Inverse of the time necessary for the disease immunity acquired from vaccination drops below critical limit |
| $\theta_R$ | Calibrated | $days^{-1}$ | Inverse of the time necessary for the acquired disease immunity without vaccination drops below critical limit |
| $\lambda$ | 1/30 | $days^{-1}$ | Inverse of the time necessary for the development of immunity through vaccination |
| $N$ | 2.09 x $10^8$ | $days^{-1}$ | Brazilian population size |

### 2.2 Bayesian calibration

Once the possible model uncertainties are accounted for the parameters of the model, the simple parameter estimation (or inference) is replaced by the Bayesian parameter inference, a process also known as Bayesian model calibration. In this intent, the robust Python probabilistic programming package pymc3 was employed (6), through the utilization of the Cascading Adaptive Transitional Metropolis in Parallel (CATMIP) algorithm (7), member of the Sequential Monte Carlo (SMC) family of techniques (8, 9). In general terms, the method consists in a population-based Monte Carlo method that relies in the iterative process of sampling and re-sampling candidate probability distributions which will asymptotically converge the density function of the function under study, according to a simulated annealing process that will converge the transitional probability kernels to a desired probability distribution through a finite number of iterative steps (9, 10). The interested reader is referred to the works of (7, 11, 12) for the thoroughly description of the process and the underlying statistical concepts.

The Bayesian calibration process was carried out considering the parameters to be calibrated from the MOSVAC model (namely $\beta, \sigma, \gamma_I, \eta_I, \theta_R$) as stochastic parameters, whose uncertainty stems from the compromise of information due to factors such as under-reporting, lack of testing mass production on a significant scale for the population, among other factors. In general terms, the mathematical description of the process consists of calibrating the set of parameters given the observations y, thus determining the uncertainties most likely for the calibrated parameters, resulting in a posteriori probability distribution. Such a process can be described presented from a point of view stochastic in Equation 9, according to the Bayes rule (4).

$$\boldsymbol{P_p}(\boldsymbol{p} \vee \boldsymbol{y}) = \boldsymbol{P_{pr}}(\boldsymbol{p}) \frac{\boldsymbol{P_l}(\boldsymbol{y} \vee \boldsymbol{p})}{\boldsymbol{P_e}(\boldsymbol{y})} \qquad (9)$$

In the Equation 9, the terms $\boldsymbol{P_p}, \boldsymbol{P_{pr}}, \boldsymbol{P_l}, \boldsymbol{P_e}$represent respectively: the posterior probability distribution; the a priori (initially defined) probability distribution regarding $\boldsymbol{p}$, defined as uniformly distributed variables as prior knowledge; the likelihood function that measures the goodness of fit of a supposed statistical model to describe the observed data, given the model parameters; and the information encompassed in the data. Only the data regarding the positively diagnosed and deceased individuals (respectively *T* and *D* in the *MOSVAC* model) were used in the calibration, and it is assumed that the uncertainties regarding those data subsets (the stochastic parameters of the

model, namely $\boldsymbol{\beta, \sigma, \gamma_I, \eta_I, \theta_R}$) follows a Gaussian distribution with standard deviations $s_T^2$ and $s_D^2$, respectively. Hence, the likelihood function employed in the calibration process is presented in the Equation 10.

$$\boldsymbol{P_p(p \vee y) = P_{pr}(p) \frac{P_I(y \vee p)}{P_e(y)}} \qquad (10)$$

In the aforementioned equation, the parameters $\boldsymbol{p}$ represent the unobserved random variables, defined as uniformly distributed *a priori*. In a similar way, the standard-deviation presumed for the epidemiological data is also considered as a random variable, being defined empirically through the aforementioned method. The calculation of the accumulated of the data for comparison with the official epidemiological information registered for the number of diagnosed cases and deceases ($T_{TOT}$ and $D_{TOT}$, respectively) are assessed through the Equations 11-12. Those values represent the model output, which the CATMIP routine employs for the comparison with the historical data.

$$\boldsymbol{T_{TOT} = \int_{t_0}^{t_f} (\epsilon_A A + \epsilon_I I)\, dt} \quad (11)$$

$$\boldsymbol{T_{TOT} = \int_{t_0}^{t_f} (\epsilon_A A + \epsilon_I I)\, dt} \quad (12)$$

### 2.3 Establishment of immunization scenarios for study

Considering that the values for stochastic parameters of the model are determined in the form of a posterior distribution probability, using the available epidemiological data during the observed time interval, the model responses can be inferred for different values of the working variables in the context of a vaccination immunization program in the country. In the present work, the following variables were adopted: the effectiveness of immunization through vaccination $(\Psi)$, which may be affected by the lacking of immunizing agent for application of two doses treatment when necessary, or improper handling of those; daily individual immunization rate $(\Phi)$; the necessary time for the immunization conferred by the vaccination is reduced to a value below the critical limit $(\theta_V)$, causing the individual to become again susceptible to contamination. Those variables were divided into two different levels (optimistic, pessimistic), and the immunization scenarios were obtained for each one of the variables, resulting in the 8 different parameter configurations presented in the Table 2. This parametric scheme is equivalent to experimental design of two levels with two factors ($2^3$), although lacking its theoretical framework in terms of the result analysis.

The values referring to optimistic and pessimistic scenarios for the study variables are presented in the Table 3. It is worth to mention that the duration time for immunity acquired through vaccination $\left({\theta_V}^{-1}\right)$ was presented, with the intent to obtain a more informative value with unit in $days$. It is worth to mention that in the determination of the daily immunization rate $(\Phi)$, it was considered that 50% of the planned monthly produced value is made available to vaccination sites as an optimistic value, whilst the pessimistic value is assumed to be 1% of this quantitative.

The simulation of the compartmentalized model presented in the Equations 1-8 consisted in the substrate for the realization of the model calibration process, as aforementioned. All the numerical simulations were performed through the Python computational language library for numerical tasks, the scipy (16), using the function ivp_solve, that provides several integrative robust solvers for solution of the incidental initial value problems. In the present work, the LSODA routine (17) was employed in this intent, which has adaptive order variation, being referred as a reliable method for resolution of numerical stiff problems. The model parameter values presented in the Table 1 were used in the simulations. The epidemiological data employed for model calibration were obtained through CSSE (J*ohns Hopkins University Center for Systems Science and Engineering*) through its repository on *Github* platform.

**Table 2** .Immunization scenarios employed in the present work in terms of the study variable levels. The symbols *P* and *O* represent pessimistic and optimistic levels, respectively.

| Scenario number | $\Psi$ level | $\Phi$ level | $\theta_V$ level |
|---|---|---|---|
| 1 | P | P | P |
| 2 | O | P | P |
| 3 | P | O | P |
| 4 | O | O | P |
| 5 | P | P | O |
| 6 | O | P | O |
| 7 | P | O | O |
| 8 | O | O | O |

**Table 3**. Nominal values for optimistic and pessimistic scenarios for study variables

| Parameter | Optimistic value | Pessimistic value |
|---|---|---|
| 1 | 1095 $days$ (13) | 90 $days$ |
| 2 | 95% (14) | 50% (14) |
| 3 | $6.67 \times 10^{5} day^{-1}$ (15) | $6.67 \times 10^{3} day^{-1}$ (15) |

## 3. RESULTS AND DISCUSSION

### 3.1 Model calibration

The results obtained for the calibration of the stochastic model are presented in terms of the posterior probabilities of the parameters for which the uncertainties was considered, as presented in the Figures 1-5. In the simulations, it was assumed that the vaccination was started int the 331-th epidemiological day (01/22/2021).

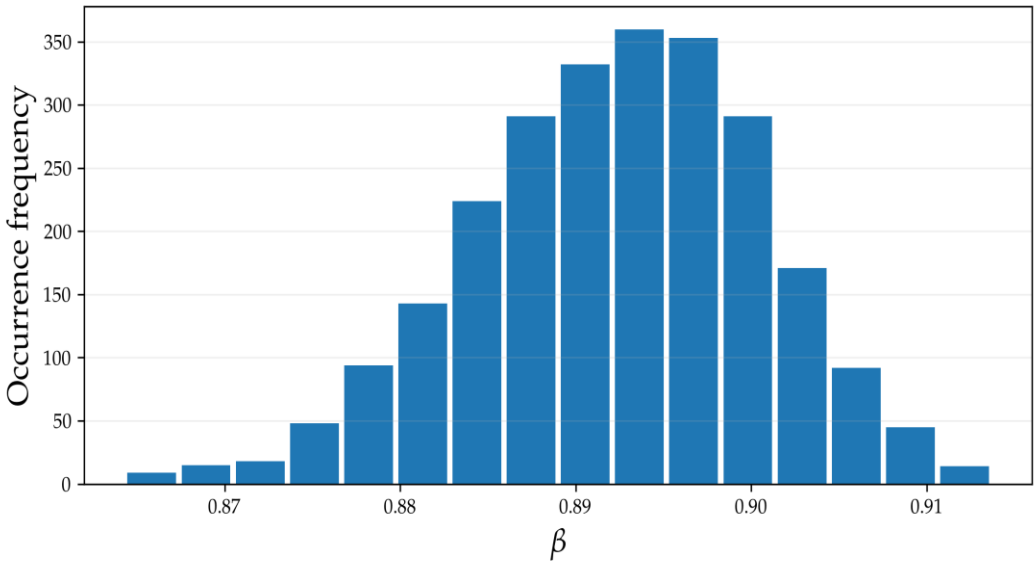


**Figure 1.** Frequency histogram for the calibrated parameter $\beta$.

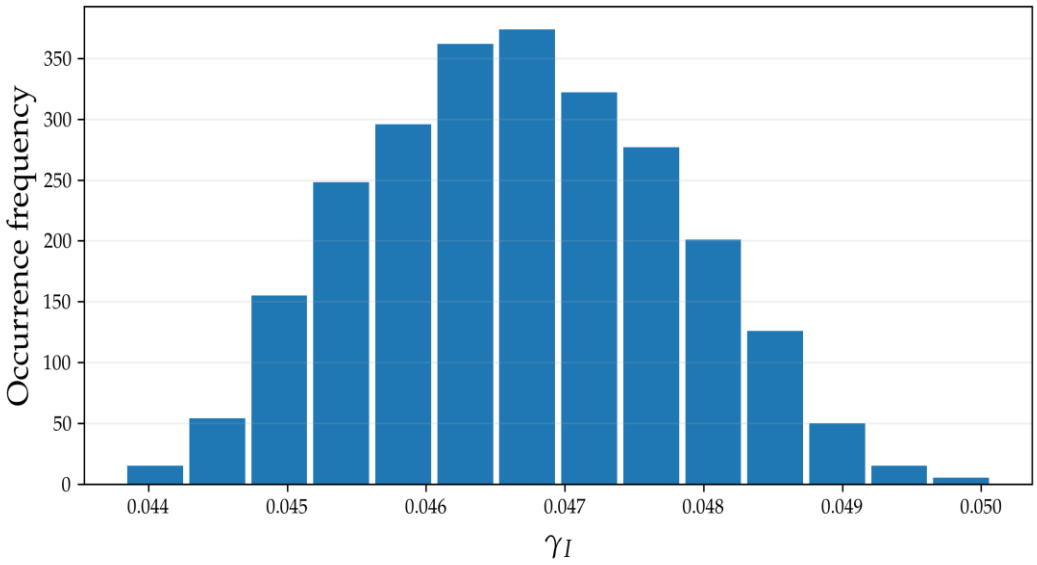


**Figure 2**. Frequency histogram for the calibrated parameter $\gamma_I$.

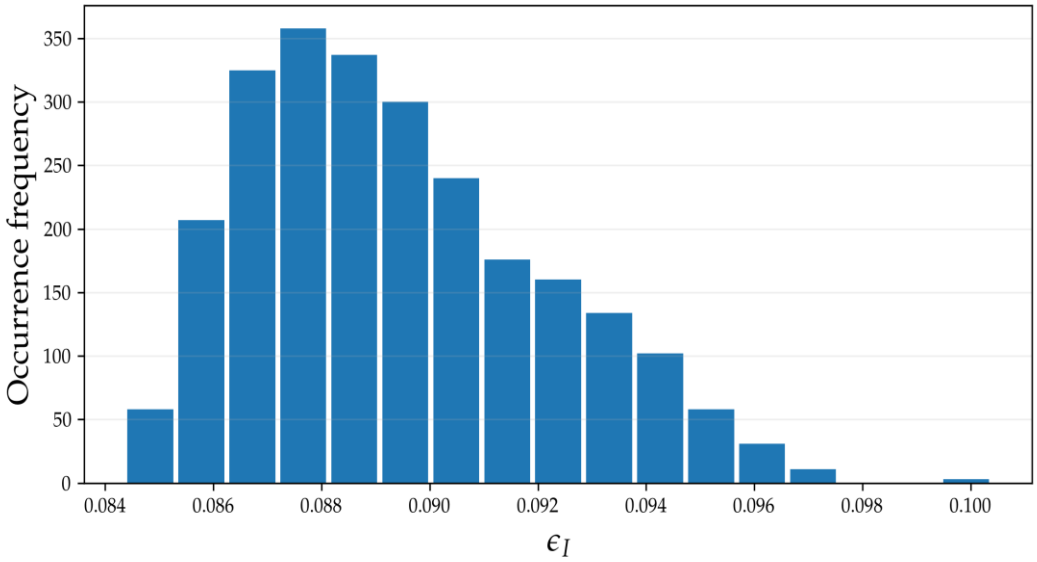


**Figure 3.** Frequency histogram for the calibrated parameter $\epsilon_I$.

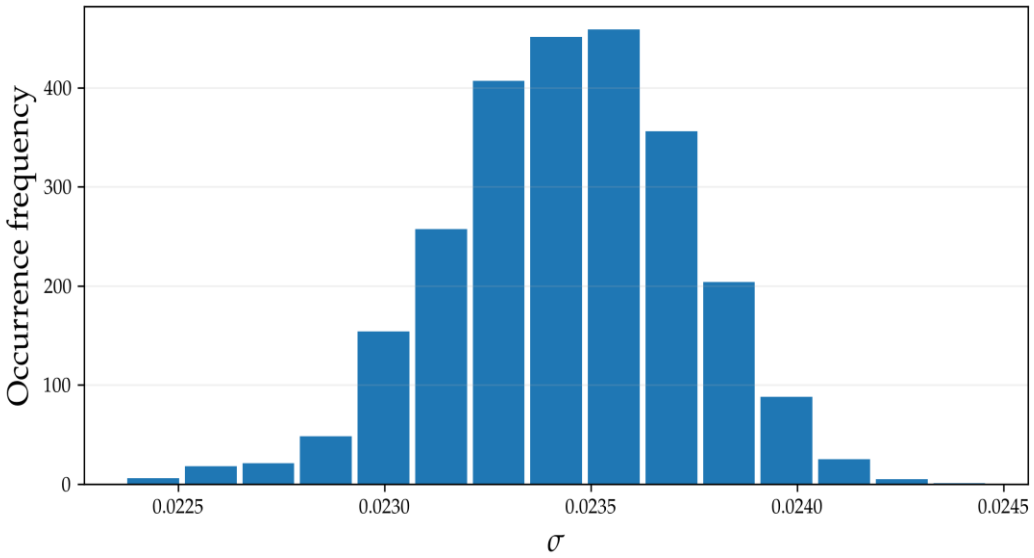


**Figure 4.** Frequency histogram for the calibrated parameter $\sigma$.

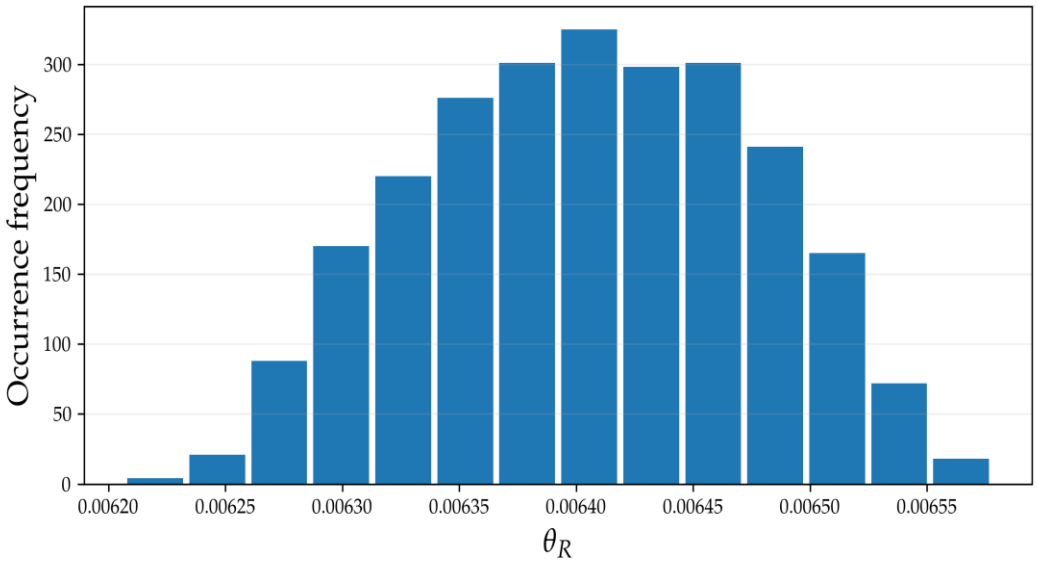


**Figure 5.** Frequency histogram for the calibrated parameter $\theta_R$.

In the Figures 1-5, it is possible to notice that the standard deviation of the calibrated parameters is relatively low, as indicated by the histograms with diminished narrow total amplitude. This fact can be explained by the fact that the model is being calibrated with a historical dataset with a large time interval (from the first detected case date in Brazil, 02/26/20, to 01/12/21), unlike the data presented in the literature (4, 18).

### 3.2 Study of the immunization scenarios

In the Figures 6-7, it is possible to observe the narrow amplitude of the obtained 95% confidence interval for the model outputs, which can be also linked to the aforementioned extension of the historical dataset used in the model calibration. The stability observed in the output for both scenario groups ($\boldsymbol{\theta_V}$optimistic and pessimistic) can be explained by the influence of the social distancing parameter ($\boldsymbol{\sigma}$), which "dampens" the impacts caused by the reduction of the duration of immunity acquired through vaccination, as well as the diminishing of the acquired immunity through disease recovery without vaccination. Nevertheless, it is important to mention that the number of disease

fatal victims can reach up to 600k individuals (circa January/2023) in the scenarios with pessimistic immunization daily rate ($\boldsymbol{\Phi}$) or vaccine effectiveness ($\boldsymbol{\Psi}$), assuming a required period of 30 days for proper development of the disease immunity through vaccination (period after which the individual can no longer be contaminated or transmit the disease) and the maintenance of the social distancing scenario assessed through the historical data.

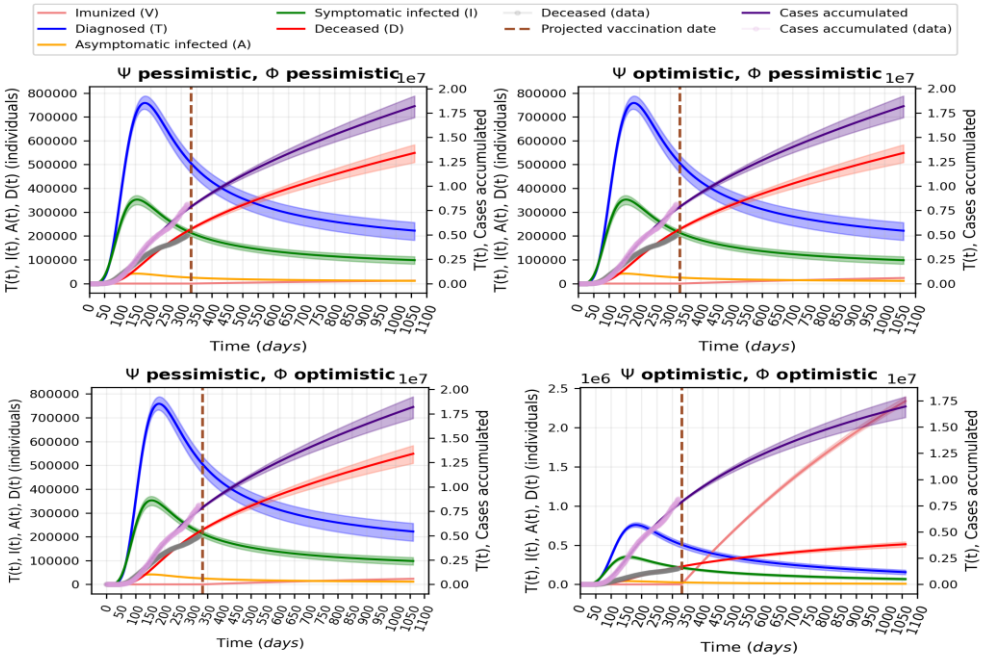


**Figure 6 .**Projected data using the *MOSVAC* model, for a optimistic $\theta_R$ scenario and multiple scenarios of $\Psi, \Phi$ (from the left to the right, and from top to bottom, scenarios number 5, 6, 7 and 8). The social distancing measures were assumed to be maintained after the start of the immunization program.

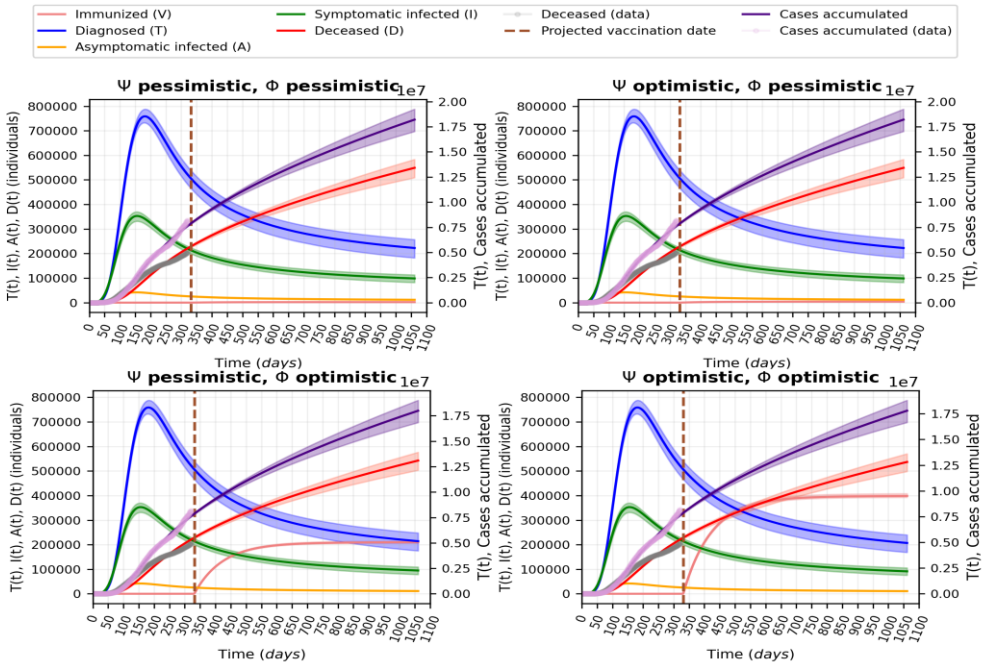


**Figure 7.** Projected data using the *MOSVAC* model, for a pessimistic $\theta_R$ scenario and multiple scenarios of $\Psi, \Phi$ (from the left to the right, and from top to bottom, scenarios number 1, 2, 3 and 4). The social distancing measures were assumed to be maintained after the start of the immunization program.

In the Figures 8-9, the results were projected for the same configuration of scenario groups (optimistic and pessimistic values for $\boldsymbol{\theta_V}$, respectively) for an abrupt removal of the social distancing measures. The projected results exhibits an expected dampened oscillatory behavior in the contamination of individuals, which led to the utilization of the more robust numerical integration method BDF (19) for projection of the scenario results. In a epidemiological sense, the oscillations obtained with the abrupt interruption of the social distancing measures represent periods of disease transmission heightening, resulting in a unbridled escalation of the individuals contaminated and deceased individuals due to COVID-19. Those results overcome significantly the benefits of the vaccination for all scenarios, even for the optimistic projection of both the immunization daily rate and effectivity.

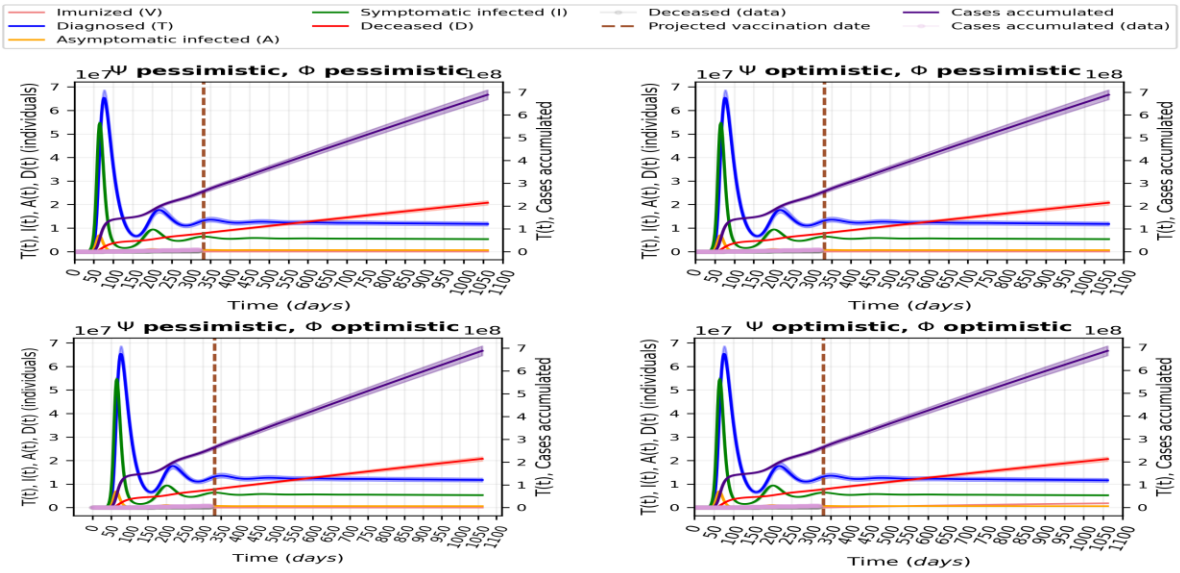


**Figure 8.** Projected data using the *MOSVAC* model, for a optimistic $\theta_R$ scenario and multiple scenarios of $\Psi, \Phi$ (from the left to the right, and from top to bottom, scenarios number 5, 6, 7 and 8). The social distancing measures were assumed to be abruptly interrupted after the start of the immunization program.

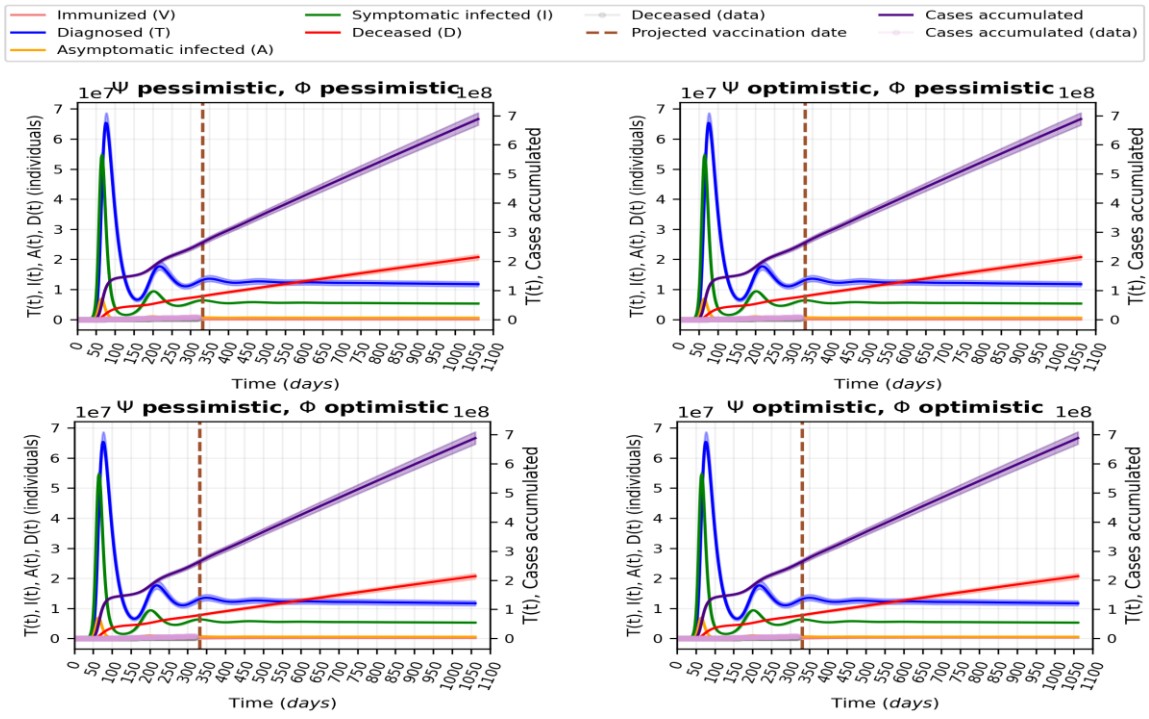


**Figure 9.** Projected data using the *MOSVAC* model, for a pessimistic $\theta_R$ scenario and multiple scenarios of $\Psi, \Phi$ (from the left to the right, and from top to bottom, scenarios number 1, 2, 3 and 4). The social distancing measures were assumed to be abruptly interrupted after the start of the immunization program.

## 4. CONCLUSION

In the present work the calibration of a compartmentalized epidemiological model with stochastic components for the COVID-19 spreading process were performed - the so called *MOSVAC* model - through the utilization of CATMIP probabilistic algorithm. The model output exhibited good agreement with the historical data, which demonstrates the algorithm robustness. It is worth to emphasize the great influence of the social distancing parameter($\sigma$)in the results obtained after the immunization program start. An abrupt interruption of the social distancing($\sigma = 0$)implies in a vertiginous escalation in both contaminated and deceased individuals numbers, exhibiting a oscillatory response that represent epidemiological cycles of reinfection. However, it is important to recognize that all mathematical models are somewhat limited, and the present projections should be considered rather in a qualitative than quantitative aspect. Despite this inherent limitation, it is evident that the Brazilian strategy for coping with the COVID-19 pandemic need to establish a massive immunization campaign with significant daily vaccination rates, which seems to be much more decisive than the vaccine effectiveness for the considered scenarios($\Psi \geq 50\%$). Ultimately, the decisive factor for a successful campaign for the disease mitigation relies in the establishment of the conjugation of responsible social distancing relaxing measures, constant with the massive immunization of the population. Only the synergy between those aspects could lead us to the proper recovery route from the nefarious effects of the pandemic in Brazil.

## CONFLICT OF INTEREST

The authors declare no conflict of interest.

### *Credit author statement*

**Hanniel Ferreira Sarmento de Freitas:** Conceptualization, Methodology, Data analysis, and Writing-Original draft preparation. **Paulo Henrique Soares:** Data analysis, Reviewing. **Cid Marcos Gonçalves Andrade:** Supervision, Reviewing.

## REFERENCES

1. JIA, Jiwei, DING, Jian, LIU, Siyu, LIAO, Guidong, LI, Jingzhi, DUAN, Ben, WANG, Guoqing and ZHANG, Ran. **Modeling the control of covid-19: Impact of policy interventions and meteorological factors.** arXiv preprint arXiv:2003.02985. 2020.

2. PENG, Liangrong, YANG, Wuyue, ZHANG, Dongyan, ZHUGE, Changjing and HONG, Liu. **Epidemic analysis of covid-19 in china by dynamical modeling.** arXiv preprint arXiv:2002.06563. 2020.

3. KUCHARSKI, Adam J, RUSSELL, Timothy W, DIAMOND, Charlie, LIU, Yang, EDMUNDS, John, FUNK, Sebastian, EGGO, Rosalind M, SUN, Fiona, JIT, Mark, MUNDAY, James D and OTHERS. **Early dynamics of transmission and control of covid-19: A mathematical modelling study.** The Lancet Infectious Diseases. 2020.

4. VOLPATTO, Diego Tavares, RESENDE, Anna Claudia Mello, ANJOS, Lucas, SILVA, Joao Vitor Oliveira, DIAS, Claudia Mazza, ALMEIDA, Regina Cerqueira and MALTA, Sandra Mara Cardoso. **Spreading of covid-19 in brazil: Impacts and uncertainties in social distancing strategies.** medRxiv. 2020. DOI 10.1101/2020.05.30.20117283.

5. CHRISTIE, Athalia, MBAEYI, Sarah A and WALENSKY, Rochelle P. *CDC interim recommendations for fully vaccinated people: An important first step*. 2021. https://www.cdc.gov/coronavirus/2019-ncov/vaccines/fully-vaccinated-guidance.html. Acessed: 2021-03-20

6. SALVATIER, John, WIECKI, Thomas V. and FONNESBECK, Christopher. **Probabilistic programming in python using PyMC3. PeerJ Computer Science [online]**. v. 2, p. e55. 2016. DOI 10.7717/peerj-cs.55. Available from: https://doi.org/10.7717/peerj-cs.55.

7. MINSON, SE, SIMONS, M and BECK, JL. **Bayesian inversion for finite fault earthquake source models i—theory and algorithm.** Geophysical Journal International. v. 194, n. 3, p. 1701–1726. 2013.

8. DOUCET, Arnaud, FREITAS, Nando and GORDON, Neil (eds.). **Sequential monte carlo methods in practice** [online]. Springer New York, 2001. Available from: https://doi.org/10.1007/978-1-4757-3437-9.

9. DEL MORAL, Pierre, DOUCET, Arnaud and JASRA, Ajay. **Sequential monte carlo samplers.** Journal of the Royal Statistical Society: Series B (Statistical Methodology). v. 68, n. 3, p. 411–436. 2006.

10. ZHOU, Yan, JOHANSEN, Adam M and ASTON, John AD. **Toward automatic model comparison: An adaptive sequential monte carlo approach.** Journal of Computational and Graphical Statistics. v. 25, n. 3, p. 701–726. 2016.

11. DOUCET, Arnaud, DE FREITAS, Nando and GORDON, Neil. An introduction to sequential monte carlo methods. In : **Sequential monte carlo methods in practice**. Springer, 2001. p. 3–14.

12. LIU, Jun S and CHEN, Rong. Sequential monte carlo methods for dynamic systems. **Journal of the American statistical association**. v. 93, n. 443, p. 1032–1044. 1998.

13. RIPPERGER, Tyler J, UHRLAUB, Jennifer L, WATANABE, Makiko, WONG, Rachel, CASTANEDA, Yvonne, PIZZATO, Hannah A, THOMPSON, Mallory R, BRADSHAW, Christine, WEINKAUF, Craig C, BIME, Christian and OTHERS. **Orthogonal sars-cov-2 serological assays enable surveillance of low-prevalence communities and reveal durable humoral immunity.** Immunity. 2020.

14. ZIMMER, Carl. *2 companies say their vaccines are 95* [online]. 2020. The New York Times. Available from: https://www.nytimes.com/2020/11/20/health/covid-vaccine-95-effective.html.

15. FIOCRUZ. [online]. 2020. Available from: https://portal.fiocruz.br/en/news/covid-19-fiocruz-will-sign-agreement-produce-vaccines-university-oxford.

16. VIRTANEN, Pauli, GOMMERS, Ralf, OLIPHANT, Travis E., HABERLAND, Matt, REDDY, Tyler, COURNAPEAU, David, BUROVSKI, Evgeni, PETERSON, Pearu, WECKESSER, Warren, BRIGHT, Jonathan, VAN DER WALT, Stéfan J., BRETT, Matthew, WILSON, Joshua, JARROD MILLMAN, K., MAYOROV, Nikolay, NELSON, Andrew R. J., JONES, Eric, KERN, Robert, LARSON, Eric, et al. **SciPy 1.0: Fundamental Algorithms for Scientific Computing in Python.** Nature Methods. v. 17, p. 261–272. 2020. DOI https://doi.org/10.1038/s41592-019-0686-2.

17. PETZOLD, LR and HINDMARSH, AC. **Lsoda.** Computing and Mathematics Research Division, I-316 Lawrence Livermore National Laboratory, Livermore, CA. v. 94550. 1997.

18. MBUVHA, Rendani and MARWALA, Tshilidzi. **Bayesian inference of covid-19 spreading rates in south africa.** PloS one. v. 15, n. 8, p. e0237126. 2020.

19. BYRNE, George D. and HINDMARSH, Alan C. **A polyalgorithm for the numerical solution of ordinary differential equations.** ACM Transactions on Mathematical Software (TOMS). v. 1, n. 1, p. 71–96. 1975.